

# Extreme Hip Motion in Professional Ballet Dancers: Dynamic and Morphologic Evaluation Based on MRI

Frank Kolo C.<sup>‡</sup> MD, Caecilia Charbonnier\* PhD, Christian W.A. Pfirrmann \*\* MD,  
Sylvain R. Duc<sup>‡</sup> MD, Anne Lubbeke<sup>†</sup> MD, Victoria B. Duthon<sup>†</sup> MD, Nadia  
Magnenat-Thalmann\* PhD, Pierre Hoffmeyer<sup>†</sup> MD, Jacques Menetrey<sup>†</sup> MD and  
Christoph D. Becker<sup>‡</sup> MD

<sup>‡</sup>*Department of Radiology, University Hospital of Geneva, Geneva, Switzerland*

<sup>\*</sup>*MIRALab, University of Geneva, Geneva, Switzerland*

<sup>\*\*</sup>*Department of Radiology, University Hospital Balgrist, Zürich, Switzerland*

<sup>†</sup>*Department of Orthopaedic Surgery, University Hospital of Geneva, Geneva, Switzerland*

---

## ABSTRACT

**Objective.** To determine the prevalence of femoroacetabular impingement (FAI) of the cam or pincer type based on magnetic resonance (MR) imaging in a group of adult female professional ballet dancers, and to quantify in-vivo the range of motion (ROM) and congruence of the hip joint in split position.

**Materials and Methods.** Institutional review board approval and informed consent from each volunteer were obtained. 30 symptomatic or asymptomatic adult female professional ballet dancers (59 hips) and 14 asymptomatic non-dancer adult women (28 hips, control group) were included in the present study. All subjects underwent MR imaging in supine position, while for the dancers additional images were acquired in split position. Labral abnormalities, cartilage lesions, and osseous abnormalities of the acetabular rim were assessed at six positions around the acetabulum. A morphological analysis, consisting in the measurement of the  $\alpha$  angle, acetabular depth and acetabular version, was performed. For the dancers, ROM and congruency of the hip joint in split position were measured.

**Results.** Acetabular cartilage lesions greater than 5 mm were significantly more frequent in dancer's hips compared to control hips (28.8% vs. 7.1%,  $p=0.026$ ), and were mostly present at the superior position in dancers. Distribution of labral lesions between the dancers and the control group showed substantially more pronounced labral lesions at the superior, posterosuperior and anterosuperior positions in dancers (54 lesions in 28 dancer's hips vs. 10 lesions in 8 control hips). Herniation pits were found significantly more often ( $p=0.002$ ) in dancer's hips ( $n=31$ , 52.5%), 25 of them being located in superior position. A cam type morphology was found for one dancer and a retroverted hip was noted for one control. Femoroacetabular subluxations were observed in split position (mean: 2.05 mm).

**Conclusion.** The prevalence of typical FAI of the cam or pincer type was low in this selected population of professional ballet dancers. The lesions' distribution, mostly superior, could be explained by a "pincer-like" mechanism of impingement with subluxation in relation to extreme movements performed by the dancers during their daily activities.

---

## KEYWORDS

Hip, early hip osteoarthritis, impingements, dancing

## **INTRODUCTION**

Professional ballet dancers' hips are subject to extreme ranges of motion (ROM) during their daily activities. ROM of the hip joint assuming extreme positions, especially while doing the splits, have not yet been determined. Furthermore, it is unclear whether the femoral head and acetabulum are congruent in these extreme positions regularly assumed by dancers. Joint incongruence could be a potential cause of early osteoarthritis (OA).

Femoroacetabular impingement (FAI) occurs when there is an abnormal contact between the proximal femur, typically the anterosuperior femoral head neck junction, and the acetabular rim. As already described before [1-7], FAI is the result of femoral or acetabular morphological abnormalities. FAI of the cam or pincer type is believed as being a potential mechanism for the development of early OA for most nondysplastic hips [8]. The study of professional ballet dancers' hips while doing the splits provides us with a potential extreme model of cam/ pincer -FAI, because of extreme flexion in that position.

Cam/ pincer -FAI, as well as subluxation (i.e., a loss of joint congruence) could be a potential cause for the development of hip pain and OA in this selected population with potential stigmata of FAI and/ or subluxation in the symptomatic dancers. Thus, the purpose of this study was to determine the prevalence of FAI of the cam or pincer type based on Magnetic Resonance Imaging (MRI) in a group of symptomatic and asymptomatic adult female professional ballet dancers. Moreover, this study aimed at quantifying in-vivo the ROM and congruence of the hip joint in extreme flexion, using MRI and computer-assisted techniques.

## **MATERIALS AND METHODS**

### **Subjects**

We conducted a cross-sectional comparative prospective study performing fifty-nine hip MRIs in thirty consecutive symptomatic or asymptomatic adult female professional ballet dancers (mean age, 24.6 years; age range, 18-39 years) and 28 control MRIs in a group of fourteen asymptomatic non-dancer adult women (mean age, 27.1 years; age range, 20-34 years). The volunteers were recruited from March to November 2007. They were excluded if they reported a prior surgery of the hip or if they presented any usual contraindication of MRI. All dancers had been dancing for more than 10 years

and practiced for more than 12 hours per week. The study was approved by our Institutional Review Board and informed consent was obtained from each volunteer.

### Outcomes of interest

The following outcomes were evaluated among the dancers and the control group: (1) Prevalence of FAI of cam or pincer type; (2) Acetabular cartilage lesions; (3) Labral lesions; and (4) Herniation pits. For the dancers, the range of motion and the congruity of the hip joint in extreme flexion were also assessed.

### MR Imaging and 3D Reconstruction

MR imaging was performed with a 1.5-T system (Avanto; Siemens Medical Solutions, Erlangen, Germany). A flexible surface coil was used. The hips of the dancers and control group were scanned in the supine position. For the dancers, additional images were acquired in split position (Fig. 1). Since this selected population of ballerinas was professional dancers, many of them having no complaints, no articular contrast media injection was performed because of the invasiveness of this procedure.



**Fig. 1** A ballet dancer in split position before MR imaging

In the supine position, a transverse 3D fast gradient echo sequence (VIBE), a coronal T1 weighted turbo spin-echo sequence, a coronal intermediate-weighted fast spin-echo sequence with fat saturation, a radial intermediate-weighted fast spin-echo sequence with fat saturation using the long axis of the femoral neck as a rotation center, and a sagittal water excitation three-dimensional double-

echo steady state sequence were performed. While doing the splits, a sagittal water excitation three-dimensional double-echo steady state sequence and a transverse 3D fast gradient echo sequence (VIBE) were achieved. Table 1 details the imaging parameters of each MRI sequence.

Using the MR images in supine position, a virtual 3D model of the hip joint was reconstructed utilizing a validated segmentation software [9-10]. Thus, for each volunteer, patient-specific 3D models of the pelvis and femur were obtained. The average (standard deviation) accuracy of this reconstruction was 1.25 mm ( $\pm 1$  mm) [9-10].

### Image Analysis

Two experienced musculoskeletal radiologists (with 6 and 14 years of experience in musculoskeletal radiology, respectively) analyzed all MR images in consensus with a randomized patient's order. The readers were blinded to the clinical evaluation.

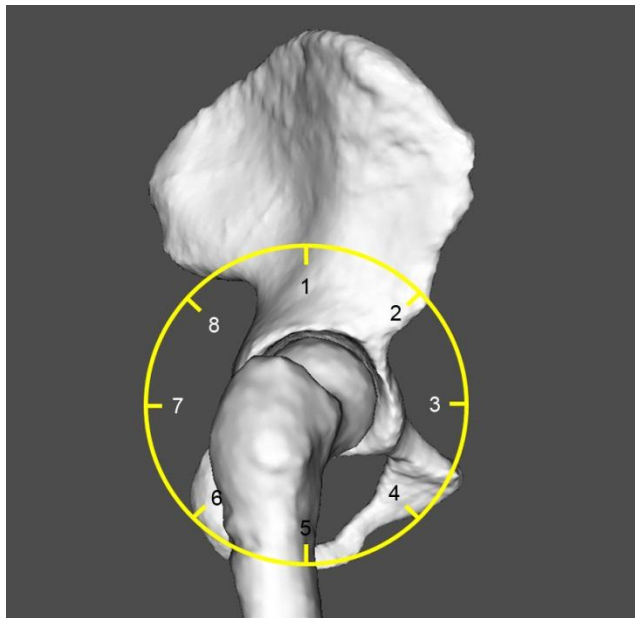


**Fig. 2** Acetabulum divided into 8 sectors (position 1, superior; position 2, anterosuperior; position 3, anterior; position 4, anteroinferior; position 5, inferior; position 6, posteroinferior; position 7, posterior; position 8, posterosuperior). The acetabular cartilage abnormalities, the labral abnormalities, and the acetabular bony contours were assessed qualitatively at positions 1 to 3 and 6 to 8.

The acetabular cartilage abnormalities, the labral abnormalities, and the acetabular bony contours were assessed qualitatively at six positions (1, superior; 2, anterosuperior; 3, anterior; 6, posteroinferior; 7, posterior; 8, posterosuperior), as depicted in Figure 2. Cartilage lesions were considered as absent or present, and extent of cartilage damage was reported in millimeter. The acetabular labrum was considered as normal, degenerated (abnormal signal intensity), torn (abnormal

linear intensity extending to the labral surface), as ossification of the labrum (continuity of the labrum with acetabular bone marrow), or as a separated ossicle (os acetabuli). The presence of subchondral acetabular or femoral bony abnormalities (e.g., edema, cysts) and the presence of a herniation pit (a round cystic lesion at the anterior aspect of the femoral neck) were also reported.

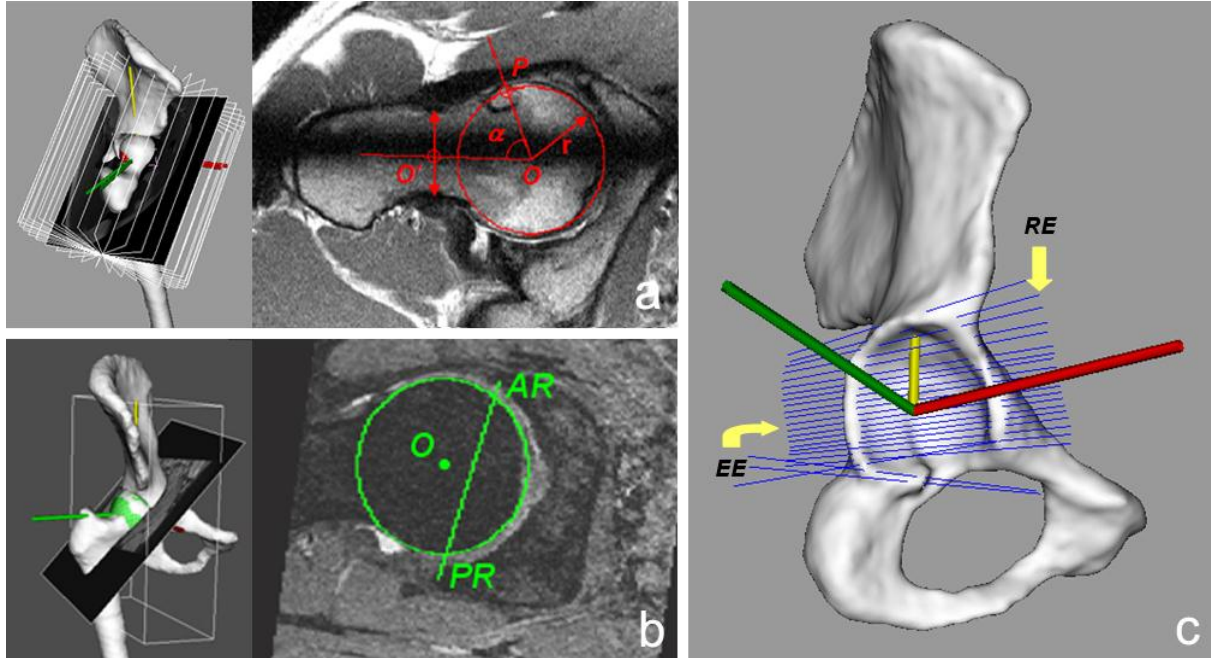


**Fig. 3** a) Definition of the  $\alpha$  angle on a radial MR image (radial intermediate-weighted fast spin-echo sequence with fat saturation, 2180/13) according to (11), illustrating a cam type morphology ( $\alpha = 85^\circ$ ). The  $\alpha$  angle is defined by the angle formed by the line  $O-O'$  connecting the center of the femoral head ( $O$ ) and the center of the femoral neck ( $O'$ ) at its narrowest point, and the line  $O-P$  connecting  $O$  and the point  $P$  where the distance between the bony contour of the femoral head and  $O$  exceeds the radius ( $r$ ) of the femoral head. b) Definition of the acetabular depth on a transverse oblique MR image (True Fisp, 10.74/4.8, flip angle 28°) obtained through the center of the femoral neck according to (2). The depth is defined by the distance between the center of the femoral neck ( $O$ ) and the line  $AR-PR$  connecting the anterior ( $AR$ ) and posterior ( $PR$ ) acetabular rim. c) Computation of the acetabular version based on 3D reconstruction; roof edge ( $RE$ ) and equatorial edge ( $EE$ ) are lines drawn between the anterior and posterior acetabular edges, defining the orientation of the acetabular opening proximally and at the maximum diameter of the femoral head respectively (arrows)

The evaluation of the waisting of the cervico-cephalic junction (femoral  $\alpha$  neck angle) and the assessment of the acetabular depth and version were performed by a third reader (with 4 years of experience in musculoskeletal radiology). The  $\alpha$  angle was measured in eight positions around the femoral neck (see Fig. 2) using radial plane images centered on the femoral neck axis [11] and superimposed on the 3D reconstructed bony models (Fig. 3a). The  $\alpha$  angle measurement was performed in accordance with the method described by Notzli et al. [12]. Deviation from the normal geometry was associated with larger  $\alpha$  angles ( $> 55^\circ$ ). The acetabular depth was evaluated according to the method detailed by Pfirrmann et al. [2]. The depth was considered as positive and normal if the center of the femoral head was lateral to the line connecting the anterior and posterior acetabular rim

(Fig. 3b). Measurement of the acetabular version was based on the angle between the sagittal direction and lines drawn between the anterior and posterior acetabular rim, at different heights (Fig. 3c). The angle was considered as positive when inclined medially to the sagittal plane (anteversion) and negative when inclined laterally to the sagittal plane (retroversion).

### Extreme ROM and Joint Congruency Computation

Extreme ROM of the hip joint were calculated using the 3D bony models derived from the dancers' MRI data and two coordinate systems (one for the femur and one for the pelvis). We used the definitions proposed by the Standardization and Terminology Committee of the International Society of Biomechanics [13] to report joint motion in an intra- and inter-subject repeatable way. The local axis system in each articulating bone was first generated. This was achieved by setting a geometric rule that constructed the pelvic and femoral coordinate systems using selected anatomical landmarks defined on the reconstructed surface of the hip and femur bones. These axes then standardized the joint coordinate system (Fig. 4a). In the neutral position and orientation, the pelvic and femoral frames were aligned. Thus, given the extracted bone positions from MR images in split position, the relative orientation between the hip bone and femur was determined by computing the relative orientation of the femoral frame to the pelvic frame (Fig. 4b). This was finally expressed in clinically recognizable terms (flexion/ extension, abduction/ adduction and internal/ external rotation) by representing the relative orientation as three successive rotations. It is important to note that the measurements were performed independently of the major anatomical planes (i.e., sagittal, transverse, frontal planes).

Using the method described in Gilles et al. [14], the congruency of the hip joint in extreme flexion was computed as follows: the hip joint center (HJC) position was first estimated in the reference neutral posture. This was determined based on the simulation of a circumduction motion pattern applied to the 3D bony models, while enforcing a constant inter-articular distance corresponding to the reference distance in the neutral posture. For this simulated motion (involving rotation and translations), the HJC was estimated as the less moving femoral point in the pelvic frame. The 3D bony models were then registered to extract joint poses from MR images in split position. Finally, femoroacetabular translations were measured with reference to the previously estimated HJC.

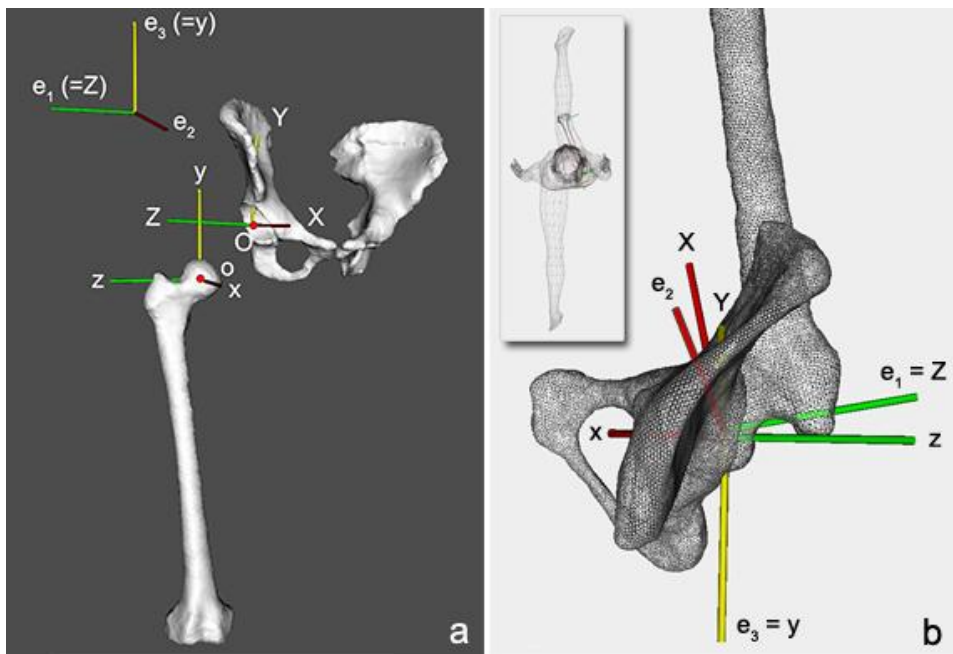


**Fig. 4** a) The pelvic coordinate system ( $XYZ$ ), the femoral coordinate system ( $xyz$ ), and the joint coordinate system ( $e_1e_2e_3$ ) for the right hip joint. Flexion/ extension is about the pelvic body fixed axis ( $e_1$ ). Internal/ external rotation is about the femoral body fixed axis ( $e_3$ ) and abduction/ adduction is about the floating axis ( $e_2$ ). b) Representation of the relative orientation between the hip bone and femur using the pelvic and femoral coordinate systems, while the subject is in split position (top view)

### Statistical Analysis

The outcomes of interest were evaluated in 59 hips (29 bilateral and 1 unilateral) of 30 dancers and in 28 hips of 14 control subjects of similar age and sex. For categorical variables, odds ratios (OR) and their 95% confidence intervals (CI) were calculated and a p-value was obtained using the chi-square or Fisher's exact test. For continuous variables, mean values and standard deviations (SD) were calculated, as well as p-values using the Mann-Whitney U test. The statistical software package SPSS, version 15.0 was employed.

## RESULTS

### Imaging Data

Based on the assessment of the MRI scans, three types of lesions were found in the dancers' hips: acetabular cartilage thinning associated with subchondral cysts (Fig. 5), degenerative labral lesions (Fig. 6), and herniation pits in superior position (Fig. 7).

Acetabular cartilage lesions greater than 5 mm were significantly more frequent in dancer's hips compared to control hips (28.8% vs. 7.1%,  $p=0.026$ ). In dancers, they were mostly present at the superior position (Table 2). Distribution of labral lesions between the dancers and the control group in

six positions around the acetabulum (Table 3) showed substantially more pronounced labral lesions at the superior, posterosuperior and anterosuperior positions in dancers (54 lesions in 28 dancer's hips vs. 10 lesions in 8 control hips). Fibrocystic changes (herniation pits, Table 4) were found significantly more often ( $p=0.002$ ) in dancer's hips ( $n=31$ , 52.5%), 25 of them being located in superior position. In the control group, pits were found in 5 hips (17.9%), 4 at the anteroinferior and 1 at the anterior position. Osseous bump formation at the femoral neck was observed for one dancer only. Subchondral acetabular cysts were noted for 2 dancer's hips, 1 being located in posterior and 1 in posterosuperior positions.

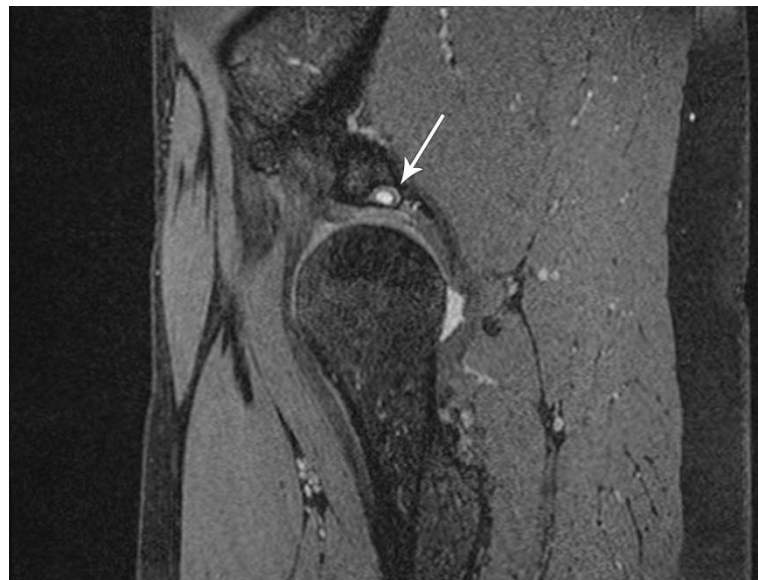


**Fig. 5** Sagittal True Fisp (10,74/4,8; 28° flip angle) MR image shows a posterosuperior acetabular cartilage defect associated with a subchondral cyst (arrow)

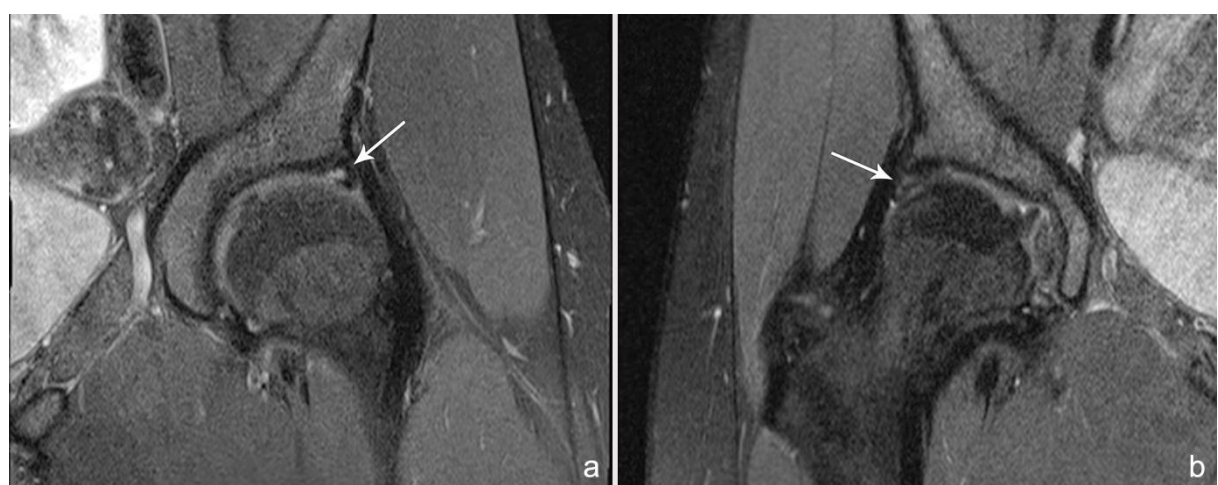


**Fig. 6** a) Coronal intermediate-weighted MR image (2180/13) with fat saturation shows an incomplete tear of the anterosuperior labrum (arrow). b) Coronal intermediate-weighted MR image (2180/13) with fat saturation shows areas of high signal intensity inside the superior part of the labrum (arrow) indicating degenerative changes

Results of the morphological measurements revealed that the dancers' and control group hips were normal, except for one dancer where a cam morphology was found in relation with the detected osseous bump formation, and for one subject in the control group where a retroverted hip was noted. Table 5 summarizes the results of our morphological analysis.



**Fig. 7** Coronal intermediate-weighted image (2180/13) with fat saturation. Note the herniation pit at the superior position of the femoral head-neck junction (arrow)

### ROM and Joint Congruency Data

As reported in Gilles et al. [14], the 59 hip MRI of dancers while doing the splits showed a mean femoroacetabular subluxation of 2.05 mm (range 0.63 - 3.56 mm). We did not observe any privileged direction of femoroacetabular translations. For the ranges of motion, the angles showed low standard deviations, suggesting that movements were repeated similarly across dancers. No significant left-right differences were noted. Table 6 reports the computed ROM and subluxation of the hip joint in extreme flexion.

### DISCUSSION

According to the clinical examination performed by two experienced orthopedic surgeons, the majority of dancers complained of hip pain while dancing only [15]. 55% of the dancers had pain and lesions on MRI, while 35% had no pain and lesions on MRI. Some dancers (5%) had pain but no lesions on MRI. The authors therefore concluded that no clear correlation between clinical and radiological findings could be done [15]. As demonstrated by the morphological analysis and distribution of lesions in dancers' hips, typical FAI are low in this selected population of professional ballet dancers. Indeed,

an abnormal morphology of the cam type was found in only one hip, where the characteristic findings expected in cam type FAI were observed - an osseous bump at the anterosuperior femoral head-neck junction and labro-cartilaginous lesions located along the anterosuperior part of the acetabulum. Moreover, when analyzing the MR images acquired in split position, it is interesting to note that the herniation pits were exactly located at the contact zone between the anterosuperior femoral head-neck junction and the acetabulum, as expected in case of cam type FAI (see Fig. 8).

Despite the absence of articular contrast media injection which could lower the sensitivity and specificity of cartilaginous and labral detection, hip lesions of the acetabular labrum and cartilage, as well as the herniation pits, were for the majority of dancers statistically more pronounced at the superior position around the acetabular rim compared to the group of asymptomatic non-dancer female volunteers. Acetabular cartilage lesions greater than 5 mm were significantly more frequent in dancers (28.8% vs. 7.1%,  $p=0.026$ ) and were mostly present at the superior position. Distribution of labral lesions between the dancers and the control group in six positions around the acetabulum showed substantially more pronounced labral lesions at the superior, posterosuperior and anterosuperior positions in dancers (54 lesions in 28 dancer's hips vs. 10 lesions in 8 control hips). Herniation pits were found significantly more often ( $p=0.002$ ) in dancer's hips ( $n=31$ , 52.5%), 25 of them being located in superior position. This pattern of lesions' distribution has to our knowledge not been reported in typical FAI of the cam or pincer type. In the absence of a focal or global acetabular overcoverage such as a prominent posterior acetabular wall, acetabular retroversion, coxa profunda or protrusio acetabuli, the explanation for the presence of these lesions seems to be their correlation with extreme motion assumed by the dancers' hips during their daily activities. These extreme positions seem to be responsible for a "pincer-like" mechanism of impingement with linear contact between the superior or posterosuperior acetabular rim and the femoral head-neck junction. This mechanism has been demonstrated by Charbonnier et al. [16-17] who assessed dynamically the dancers' hip joints motion. Dynamic data were collected by these authors, while the professional dancers were performing 6 dancing movements: arabesque, développé devant, développé à la seconde, grand écart facial, grand écart latéral and grand plié. Visualization of the hip motion and functional evaluation were based on dancer-specific 3D models obtained by the segmentation of MRI data and the use of optical motion capture. The authors demonstrated that for almost all the assessed movements aforementioned, the impingement, in other words the abnormal contact between the proximal femur

and acetabular rim, was mainly located in the superior or posterosuperior quadrant of the acetabulum. From a morphological point of view, this mechanism is also supported by the fact that some dancers presented cortical irregularity in the superolateral part of the femoral neck (see Fig. 9).

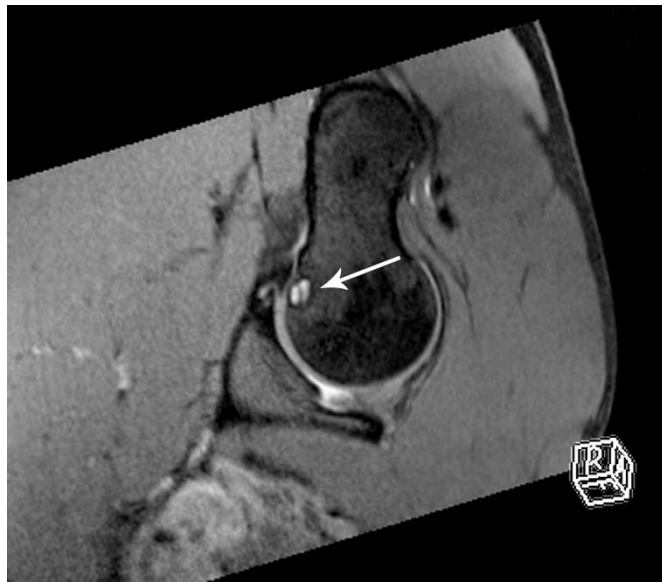


**Fig. 8** Reformatted True Fisp (10,74/4,8; 28° flip angle) MR image in a dancer being in split position. Note the herniation pit located at the contact zone between the anterosuperior femoral head-neck junction and the acetabulum (arrow)



**Fig. 9** Coronal T1-weighted (565/13) MR image. Note the cortical irregularity in the superolateral part of the femoral neck (arrow)

As reported in Gilles et al. [14], the MRI data acquired with the dancers in split position showed for the 59 hips a mean femoroacetabular subluxation of 2,05 mm (range 0,63 - 3,56 mm). The magnitude of subluxation during the dancing movements assessed by Charbonnier et al. [16-17] was even greater (peak value = 6,32 mm). We can thus suppose that the loss of joint congruency exposes the dancers' hips cartilage to stress which also favors cartilage lesions. Nevertheless, we must note that we did not find contrecoup lesions in the anteroinferior acetabular cartilage, as it could be expected in a "pincer-like" mechanism of impingement with subluxation. It is finally worth mentioning that those extreme movements, such as the split position performed by the dancers in the magnet bore, imply a combination of abduction, flexion and rotation.

Several study limitations need to be stated: 1) the radiological analysis that was based on hip MRI and not MR arthrography and 2) the consensus reading of the cases. In spite of these limitations, the results of our study demonstrated interesting findings which can be summarized as follows: The prevalence of typical FAI of the cam or pincer type was low in this selected population of professional ballet dancers; however, a "pincer-like" mechanism of impingement seems to occur in relation to extreme movements performed by the dancers during their daily activities. This mechanism could

explain the acetabular labral and cartilage lesions, as well as the herniation pits, predominantly found in the superior acetabular quadrant. Furthermore, femoroacetabular subluxations were observed while doing the splits. On the basis of the evidence, we believe that extreme hip motion in this selected population could be a potential risk factor for the development of early hip OA.

## **CONFLICTS OF INTEREST**

The authors declare that they have no conflict of interest.

## **REFERENCES**

1. Ganz R, Parvizi J, Beck M, Leunig M, Nötzli H, Siebenrock KA. Femoroacetabular impingement: a cause for osteoarthritis of the hip. *Clin Orthop Relat Res* 2003; 417:112-120.
2. Pfirrmann CWA, Mengardi B, Dora C, Kalberer F, Zanetti M, Hodler J. Cam and pincer femoroacetabular impingement: Characteristic MR arthrographic findings in 50 patients. *J Radiol* 2006; 240(3):778-785.
3. Beck M, Kalhor M, Leunig M, Ganz R. Hip morphology influences the pattern of damage to the acetabular cartilage: femoroacetabular impingement as a cause of early osteoarthritis of the hip. *J Bone Joint Surg Br* 2005; 87:1012-1018.
4. Ito K, Minka MA 2nd, Leunig M, Werlen S, Ganz R. Femoroacetabular impingement and the cam-effect: a MRI based quantitative anatomical study of the femoral head-neck offset. *J Bone Joint Surg Br* 2001; 83:171-176.
5. Lavigne M, Parvizi J, Beck M, Siebenrock KA, Ganz R, Leunig M. Anterior femoroacetabular impingement: Part I: Techniques of joint preserving surgery. *Clin Orthop Relat Res* 2004; 418:61-66.
6. Leunig M, Beaulé PE, Ganz R. The concept of femoroacetabular impingement. *Clin Orthop Relat Res* 2009; 467:616-622.
7. Reynolds D, Lucac J, Klaue K. Retroversion of the acetabulum: a cause of hip pain. *J Bone Joint Surg Br* 1999; 81:281-288.
8. Wagner S, Hofstetter W, Chiquet M et al. Early osteoarthritic changes of human femoral head cartilage subsequent to femoro-acetabular impingement. *Osteoarthritis Cartilage* 2003; 11:508-518.

9. Gilles B, Moccozet L, Magnenat-Thalmann N. Anatomical modelling of the musculoskeletal system from MRI. MICCAI '06, Part II. LNCS, Springer Berlin / Heidelberg, 4190, pp. 289-296, 2006.
10. Schmid J, Kim J, Magnenat-Thalmann N. Robust statistical shape models for MRI bone segmentation in presence of small field of view. *Med Image Anal* 2011; 15:155-168.
11. Rakhra KS, Sheikh AM, Allen D, Beaulé PE. Comparison of MRI alpha angle measurement planes in femoroacetabular impingement. *Clin Orthop Relat Res* 2009; 467(3):660-665.
12. Nötzli HP, Wyss TF, Stöcklin CH, Schmid MR, Treiber K, Hodler J. The contour of the femoral head-neck-junction as a predictor for the risk of anterior impingement. *J Bone Joint Surg Br* 2002; 84:556-560.
13. Wu G, Siegler S, Allard P et al. ISB recommendation on definitions of joint coordinate system of various joints for the reporting of human joint motion - part I: Ankle, hip and spine. *J Biomech* 2002; 35(4):543-548.
14. Gilles B, Kolo FC, Magnenat-Thalmann N et al. MRI-based assessment of hip joint translations. *J Biomech* 2009; 42(9):1201-1205.
15. Duthon VB, Charbonnier C, Kolo FC et al. Correlation of clinical and MRI findings in hips of elite female ballet dancers. *Arthroscopy* 2012; In Press.
16. Charbonnier C, Kolo FC, Duthon VB et al. Assessment of congruence and impingement of the hip joint in professional ballet dancers: A motion capture study. *Am J Sports Med* 2011; 39(3):557-566.
17. Charbonnier C, Kolo FC, Duthon VB et al. Professional dancer's hip: A motion capture study. *Trans Orthop Res Soc*. New Orleans, Louisiana, March 2010.

**TABLES****Table 1** MRI Sequences and their Imaging Parameters

MRI Sequence	Imaging Parameters
3D fast gradient echo (VIBE)	Section thickness 5 mm; no intersection gap; TR/TE 4.15/1.69; flip angle, 10°; field of view, 35 cm; matrix 256 × 256; one signal acquired
Coronal T1 weighted turbo spin-echo	Section thickness 3 mm; no intersection gap; TR/TE msec 565/13; flip angle 180°; field of view, 16 cm; matrix 320 × 208; one signal acquired
Coronal intermediate-weighted fast spin-echo	Section thickness 3 mm; no intersection gap; TR/TE msec 2180/13; flip angle, 180°; field of view 16 cm; matrix 320 × 224; 2 signals acquired
Radial intermediate-weighted fast spin-echo	Section thickness 3 mm; TR/TE msec 2180/13; field of view 16 cm; matrix 384 × 269; one signal acquired
Sagittal water excitation three-dimensional double-echo steady state	Section thickness 0.6 mm; TR/TE msec 10.74/4.8; flip angle 28°; field of view, 20 cm; matrix 384 × 307, one signal acquired
Sagittal water excitation three-dimensional double-echo steady state	Section thickness 1.3 mm; no intersection gap; TR/TE msec 10.74/4.8; flip angle 28°; field of view, 20 cm; matrix 384 × 384; one signal acquired
Transverse 3D fast gradient echo (VIBE)	Section thickness 5 mm; no intersection gap; TR/TE 4.15/1.69; flip angle, 10°; field of view, 35 cm; matrix 256 × 256; one signal acquired

**Table 2** Acetabular Cartilage Lesions

Position	Size of Lesion in Dancers ( <i>n</i> = 59)*			Size of Lesion in Control Group ( <i>n</i> = 28)*			OR (95% CI)	<i>P</i> Value <sup>†</sup>
	Normal	≤ 5 mm	> 5 mm	Normal	≤ 5 mm	> 5 mm		
Anterior	59	0	0	26	2	0		
Anterosuperior	53	2	4	25	2	1		
Superior	38	9	12	27	0	1		
Posterosuperior	55	1	3	28	0	0		
Posterior	57	0	2	28	0	0		
Posteroinferior	59	0	0	28	0	0		
Inferior	59	0	0	28	0	0		
Anteroinferior	59	0	0	28	0	0		
Total lesions		12	21		4	2		
Total hips (%) ≤ 5 mm		12 (20.3)			4 (14.3)		1.5 (0.4; 5.3)	0.568
Total hips (%) > 5 mm			17** (28.8)			2 (7.1)	5.3 (1.1; 24.7)	0.026

\*Data are the number of hips.

\*\*Of those 3 hips had 2 or more lesions.

<sup>†</sup> *P* values obtained with use of Fisher's exact test.

**Table 3** Labral Lesions

Position	Labrum Condition in Dancers (n = 59)*					Labrum Condition in Control Group (n = 28)*					OR (95% CI)	P Value
	Normal	Degeneration	Tear	Ossification	Ossicle	Normal	Degeneration	Tear	Ossification	Ossicle		
Anterior	52	3	3	1	0	28	0	0	0	0		
Anterosuperior	37	7	13	2	0	22	3	3	0	0		
Superior	20	18	19	2	0	12	9	3	4	0		
Posterosuperior	35	10	13	1	0	23	1	4	0	0		
Posterior	53	2	3	1	0	28	0	0	0	0		
Posteroinferior	53	2	3	1	0	28	0	0	0	0		
Inferior	57	2	0	0	0	28	0	0	0	0		
Anteroinferior	59	0	0	0	0	28	0	0	0	0		
Total lesions	34	54	8			13	10	4				
Total hips (%) Degeneration	24 (40.7)					12 (42.9)					0.9 (0.4; 2.3)	0.847†
Hips with ≥2 lesions (%)	11 (18.6)					1 (3.6)						
Total hips (%) Tear		28 (47.5)					8 (28.6)				2.3 (0.9; 5.9)	0.095†
Hips with ≥2 lesions (%)		12 (20.3)					1 (3.6)					
Total hips (%) Ossification			2 (3.4)					4 (14.3)			0.2 (0.04; 1.2)	0.082††
Hips with ≥2 lesions (%)			2 (3.4)					0				

\*Data are the number of hips.

† P values obtained with use of chi-square test.

†† P values obtained with use of Fisher's exact test.

**Table 4** Herniation Pits

Position	Herniation Pits in Dancers ( <i>n</i> = 59)*		Herniation Pits in Control Group ( <i>n</i> = 28)*		OR (95% CI)	<i>P</i> Value <sup>†</sup>
	Absent	Present	Absent	Present		
Anterior	57	2	27	1		
Anterosuperior	57	2	28	0		
Superior	34	25	28	0		
Posterosuperior	55	4	28	0		
Posterior	59	0	28	0		
Posteroinferior	58	1	28	0		
Inferior	59	0	28	0		
Anteroinferior	58	1	24	4		
Total lesions		35		5		
Total hips (%)		31** (52.5)		5 (17.9)	5.1 (1.7; 15.2)	0.002

\*Data are the number of hips.  
\*\*Of those 4 hips had 2 lesions.  
† *P* values obtained with use of Fisher's exact test.

**Table 5**  $\alpha$  Angle (degree) in Eight Positions around the Femoral Head, Acetabular Depth (mm) and Version (degree)

Measure	Dancers	Control Group	P Value <sup>†</sup>
$\alpha$ angle (anterior)	$45.5 \pm 5.3$	$47.5 \pm 4$	0.018
$\alpha$ angle (anterosuperior)	$46.7 \pm 6.7$	$46.0 \pm 4.9$	0.863
$\alpha$ angle (superior)	$40.2 \pm 4.8$	$46.6 \pm 4.4$	<0.001
$\alpha$ angle (posterosuperior)	$38.3 \pm 3.6$	$43 \pm 6.7$	
$\alpha$ angle (posterior)	$39.9 \pm 4.6$	$40.2 \pm 4.8$	
$\alpha$ angle (posteroinferior)	$38.3 \pm 3.6$	$48.7 \pm 6.9$	
$\alpha$ angle (inferior)	$40.2 \pm 3.6$	$51.2 \pm 6.3$	
$\alpha$ angle (anteroinferior)	$40.1 \pm 4.3$	$44.7 \pm 5.4$	
Acetabular depth	$7.5 \pm 1.7$	$8.7 \pm 2.1$	
Acetabular version	$7.5 \pm 4.1$	$5.9 \pm 5$	

Note: Data are mean  $\pm$  standard deviation.

<sup>†</sup> P values obtained with use of the Mann-Whitney U test.

**Table 6** ROM (degree) According to our Referential and Subluxation (mm) in Split Position

Measure	Min	Mean ± SD	Max
Flexion	109	133 ± 10	158.5
Abduction	17	32 ± 7	49
IR/ER	0 / 14.5	17.5 ± 13 / 0	41.5 / 0
Subluxation	0.63	2.05 ± 0.74	3.56